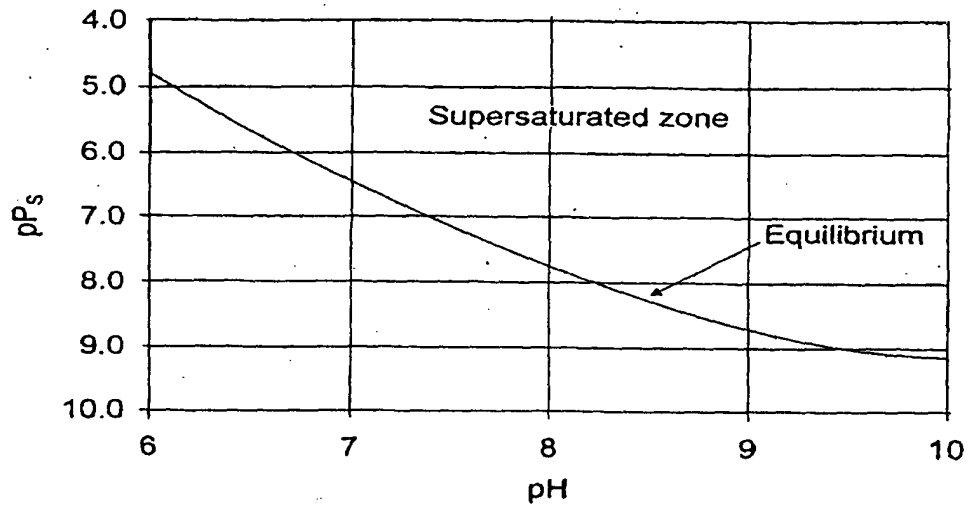

Figure 1: Variation of Equilibrium Conditional Solubility versus pH for Struvite (from Ohlinger et al., 1998)

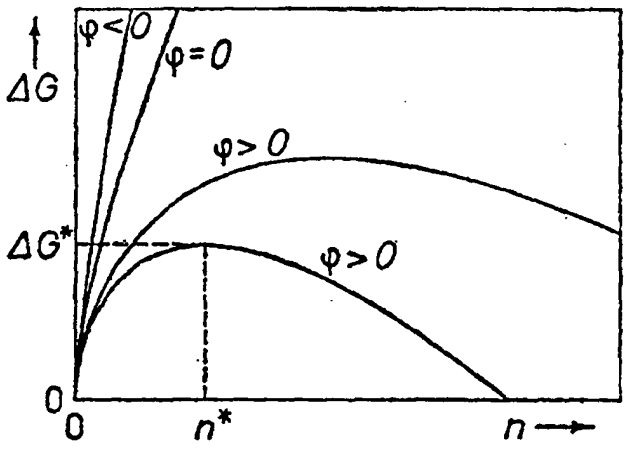

Figure 2: Free Energy versus Number of Particles in a Precipitating Crystal

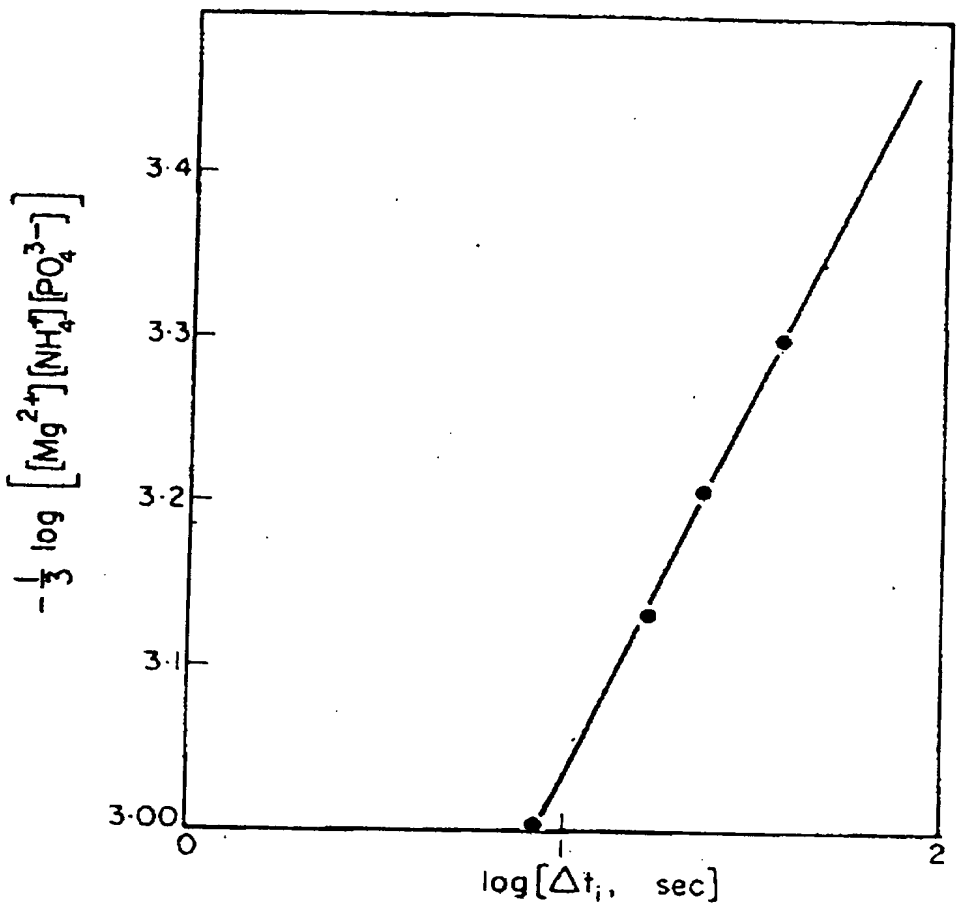

Figure 3: Concentration (-1/3 log of Ionic Product, Mol/L) versus Induction Time (Sec) for Struvite Precipitation

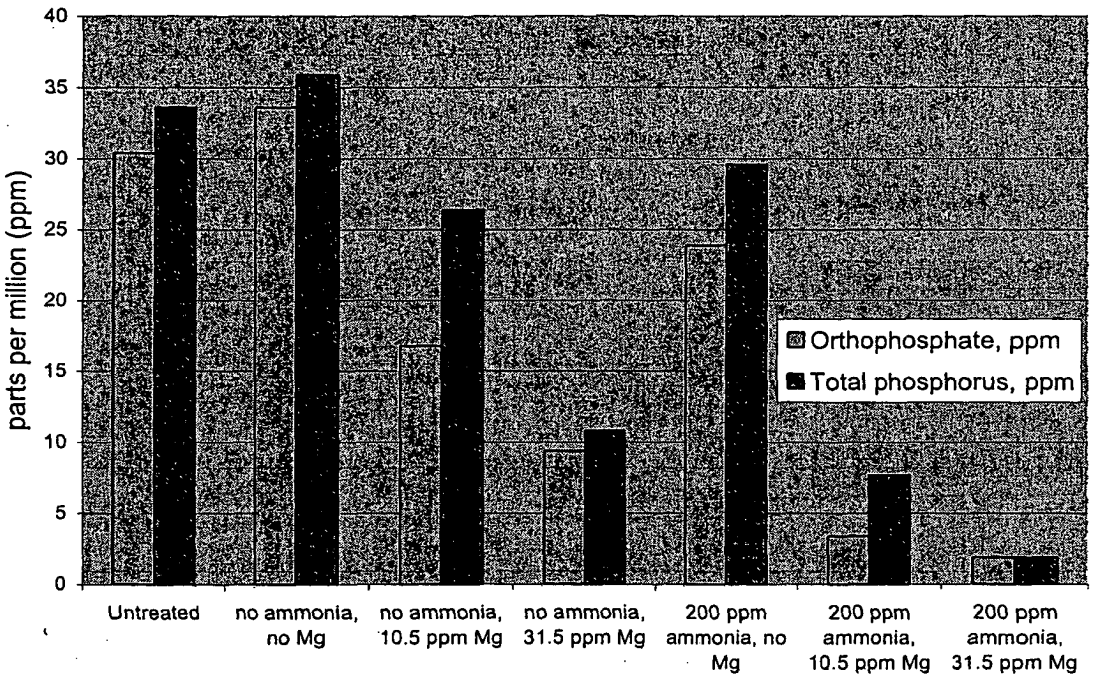

Figure 4: Dissolved OP and TP (ppm) in Untreated and Treated Effluent from Rocky Mount Lagoon

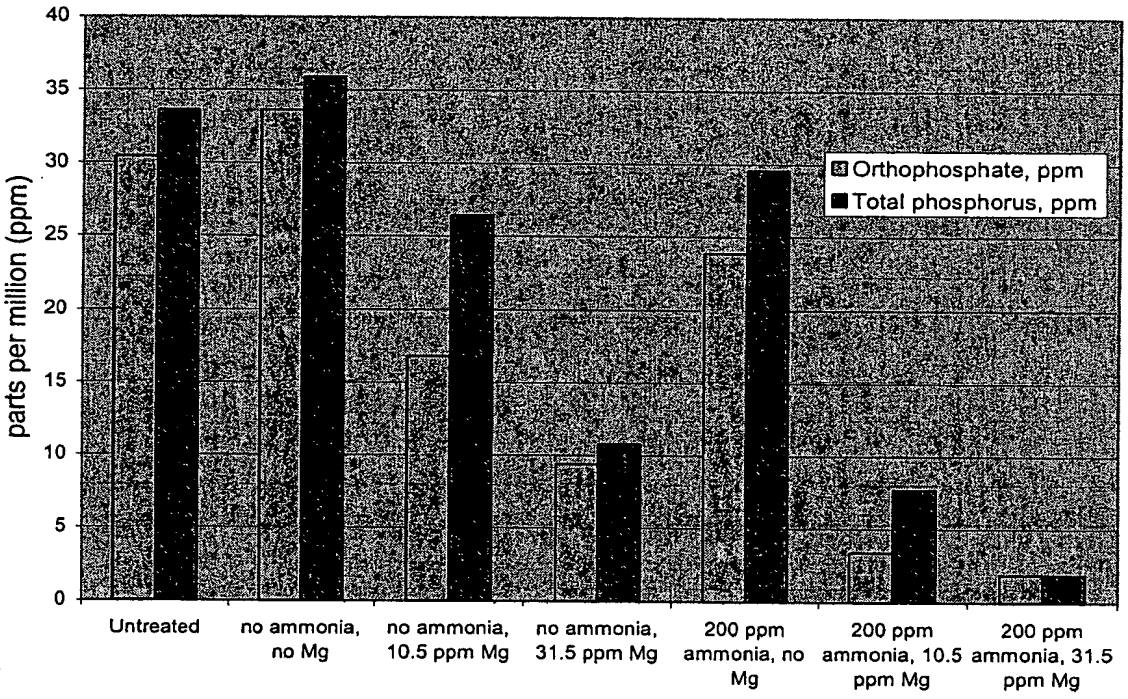

Figure 5: Dissolved OP and TP (ppm) in Untreated and Treated Effluent from Clayton Digester

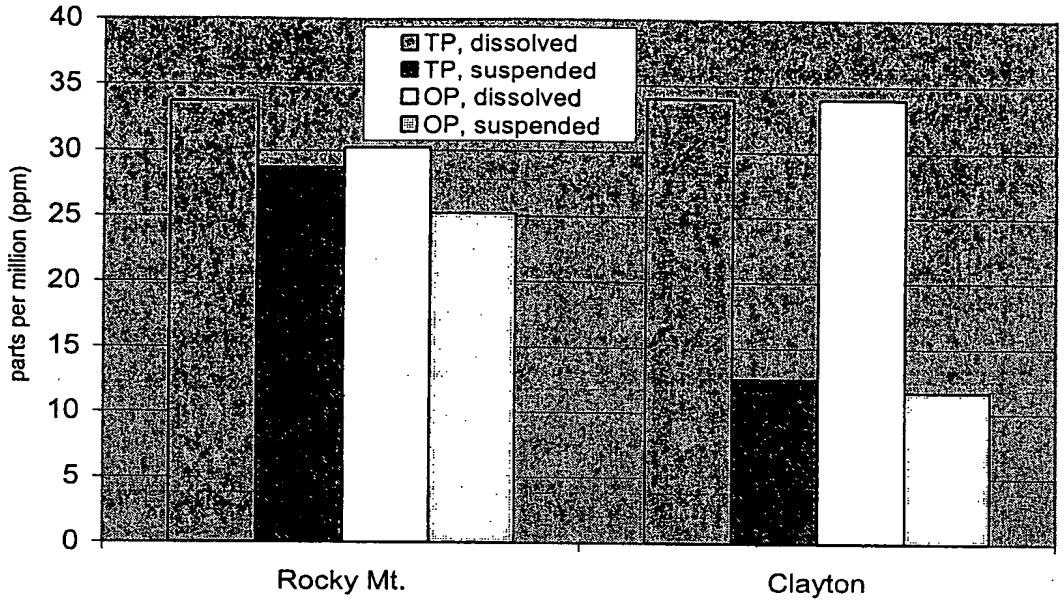

Figure 6: Breakdown of Phosphorus Content (ppm) by Form in Rocky Mount and Clayton Effluent

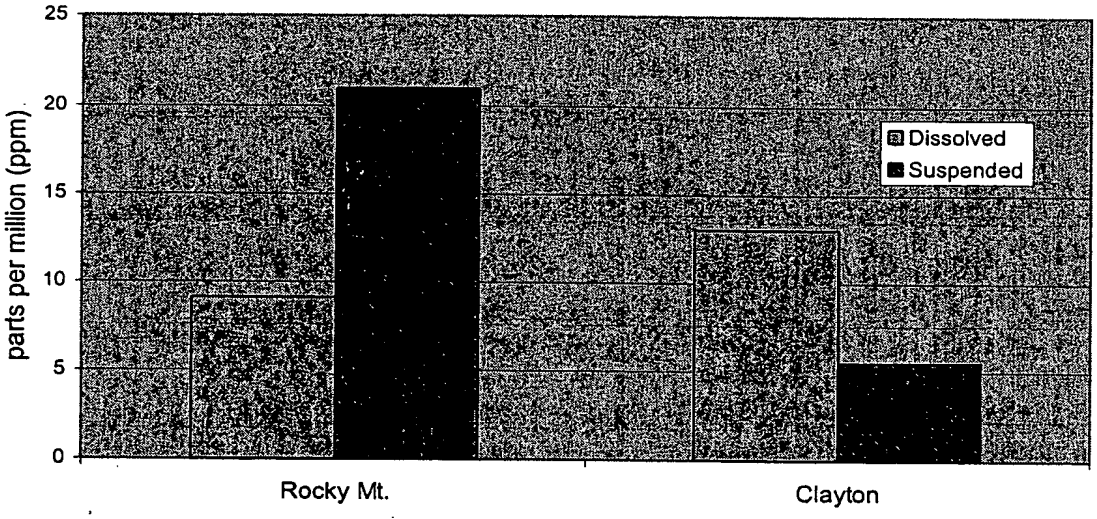

Figure 7: Breakdown of Mg Content (ppm) by Form in Rocky Mount and Clayton Effluents

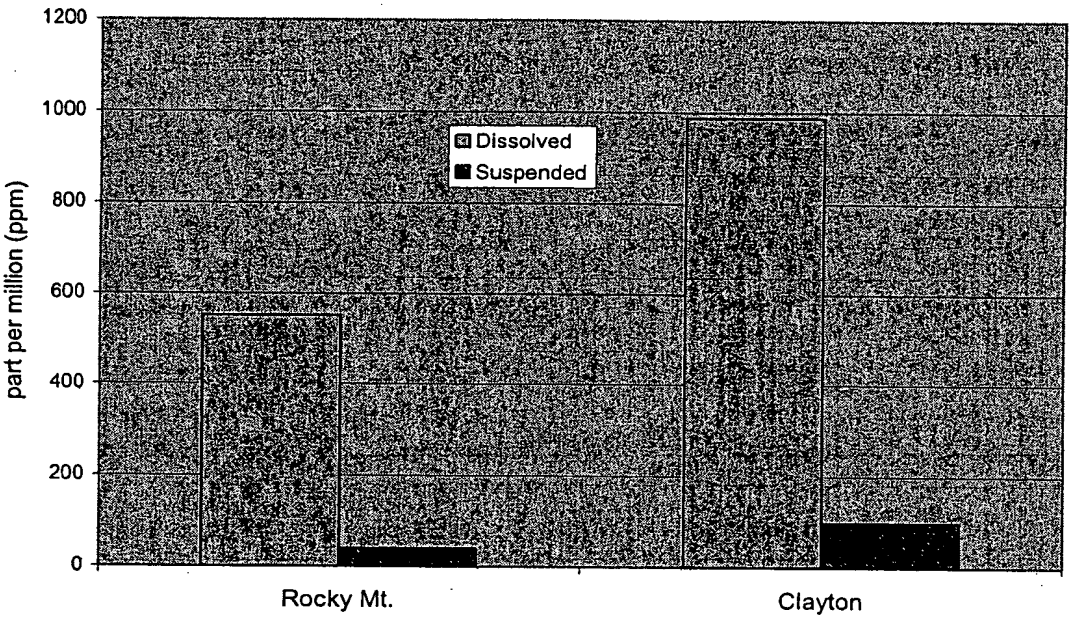

Figure 8: Breakdown of TAN (ppm) by Form in Rocky Mount and Clayton Effluent

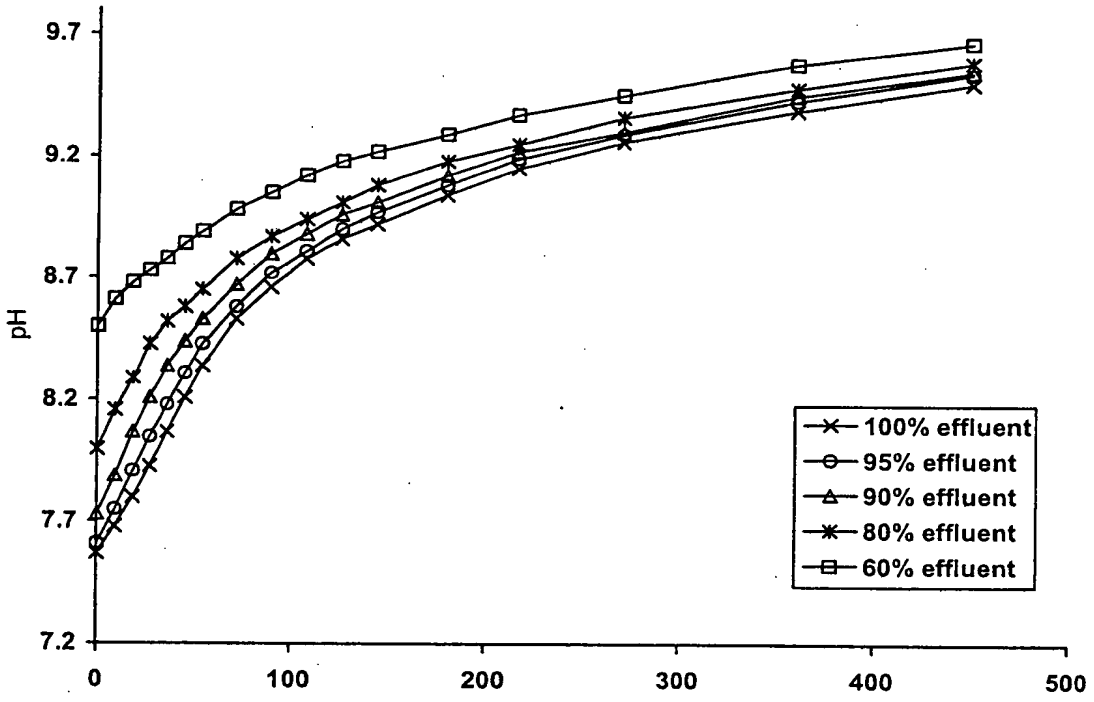

Figure 9: pH versus Amount of Ammonia Added (ppm) for Five Ratios of Effluent to Mg-Supplementing Solution

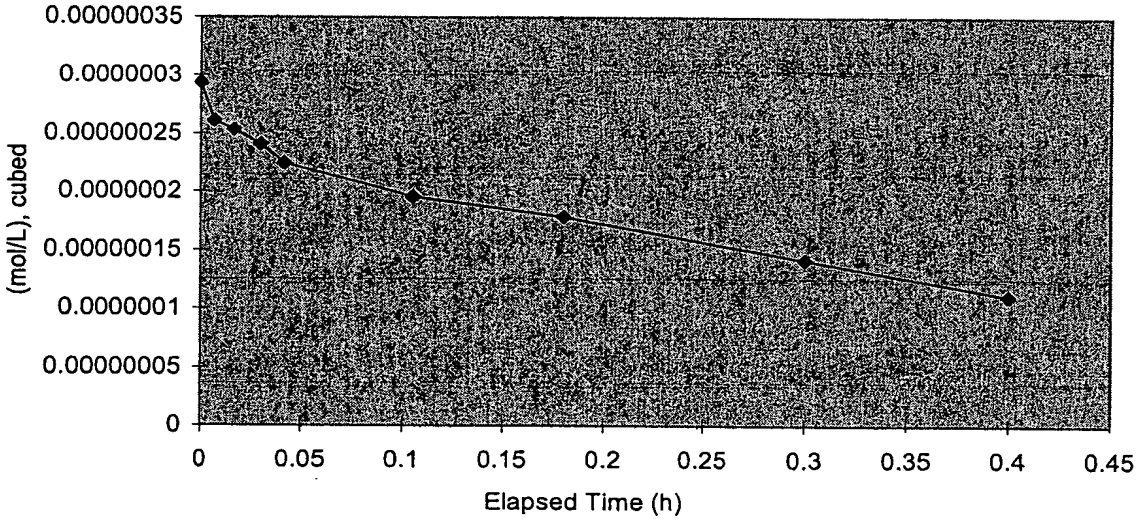

Figure 10: Excess Molar Product $(mol/L)^3$ versus Time (h) Elapsed from pH, OP, and Mg Augmentation

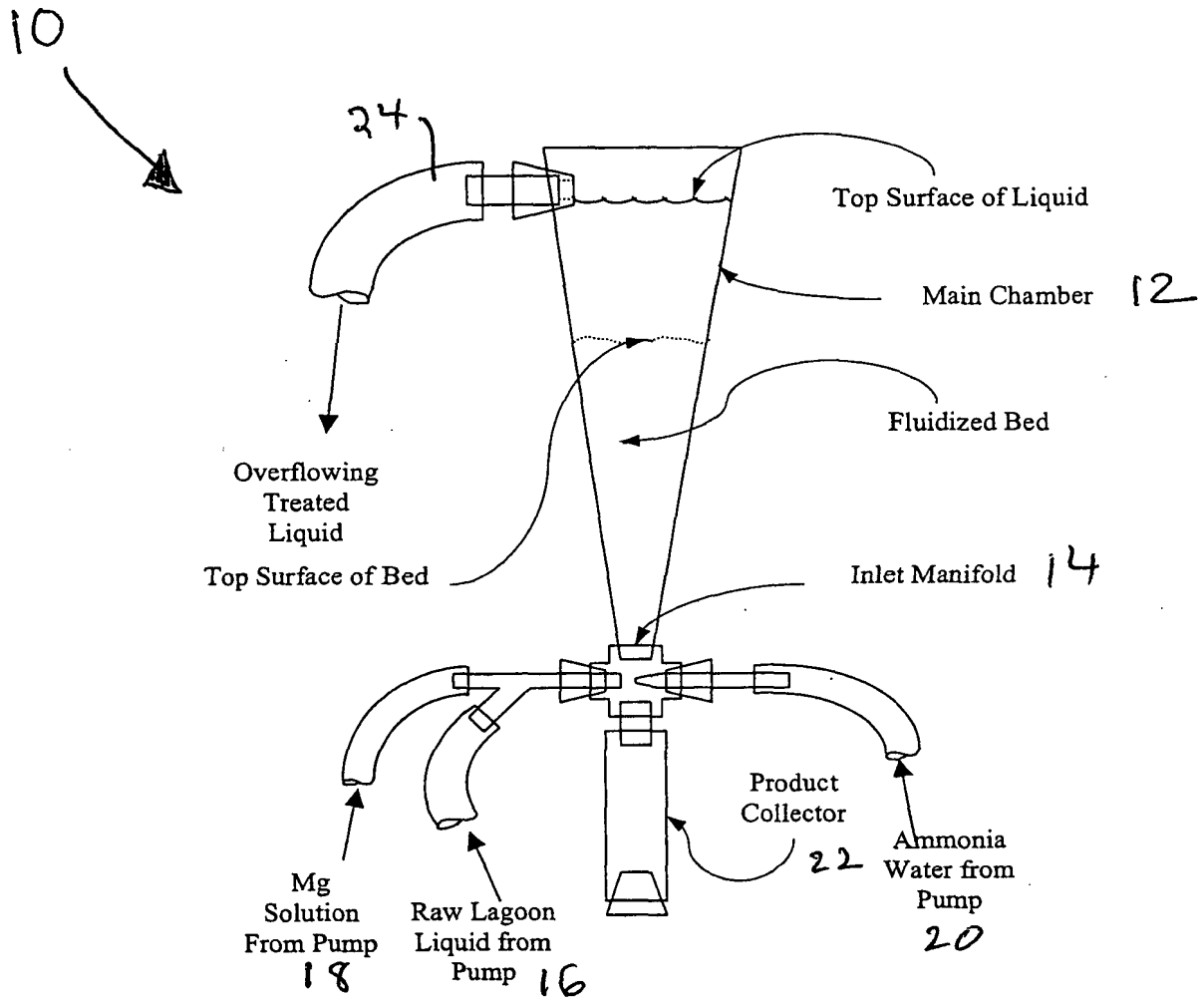

Figure 1: Sketch of Laboratory-Scale Continuous Crystallizer

Figure 11A

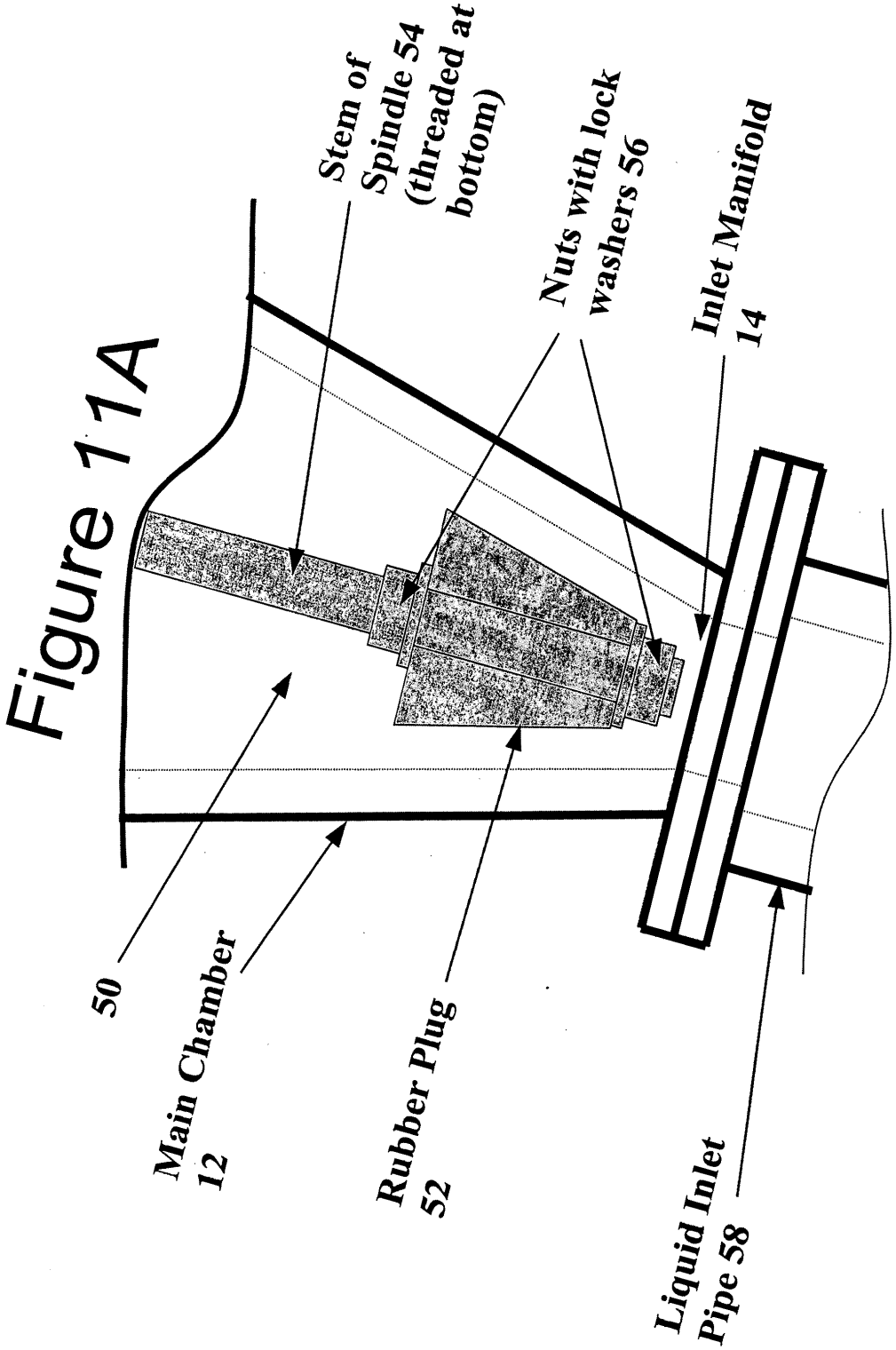
Stem of Spindle 54 (threaded at bottom)
Nuts with lock washers 56
Inlet Manifold 14
50
Main Chamber 12
Rubber Plug 52
Liquid Inlet Pipe 58

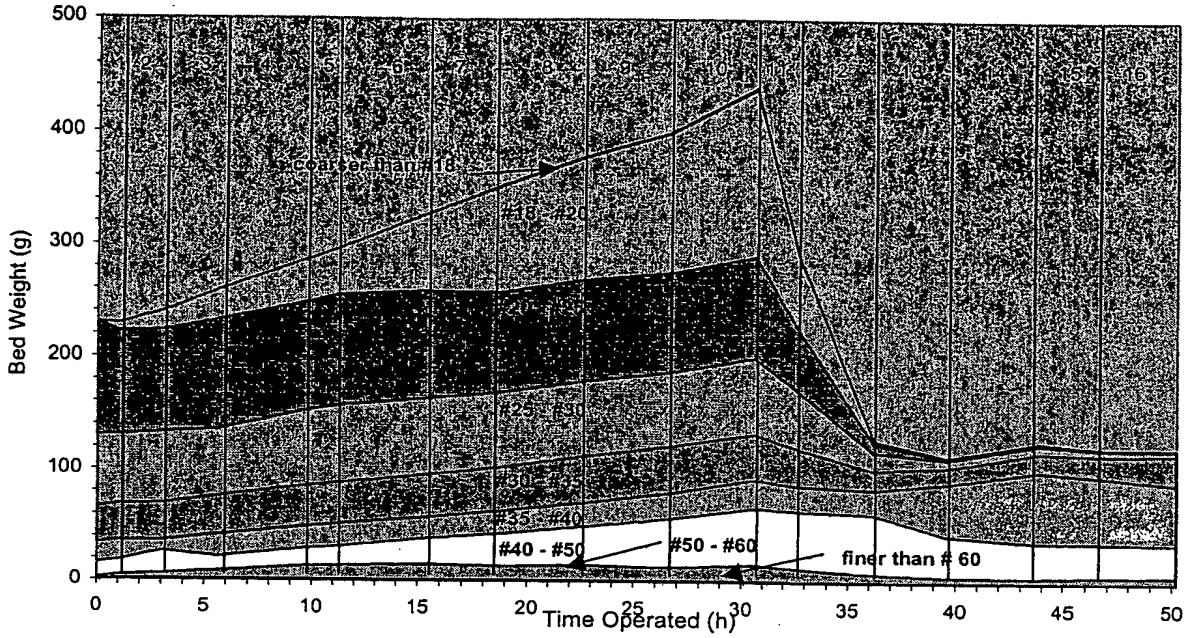

Figure 12: First Series of FCRs: Bed Weight (g), Broken Down by Particle Size (Standard Sieve), vs. Time Operated (h)
(Numbered Vertical Strips Correspond with Runs)

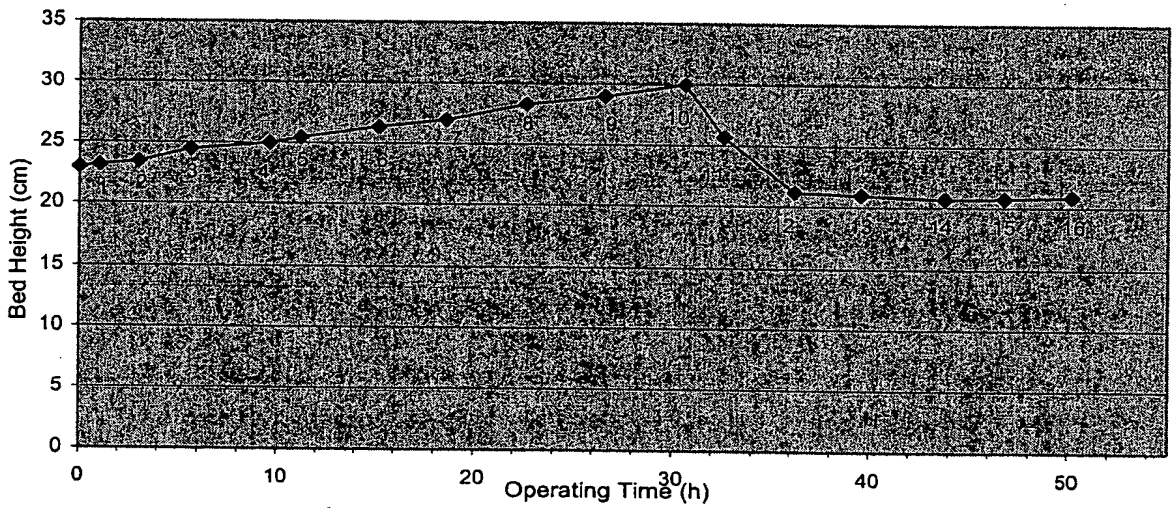

Figure 13: First Series of FCRs: Bed Height (cm) at End of Run vs. Operating Time (h)
(Run Numbers Indicated)

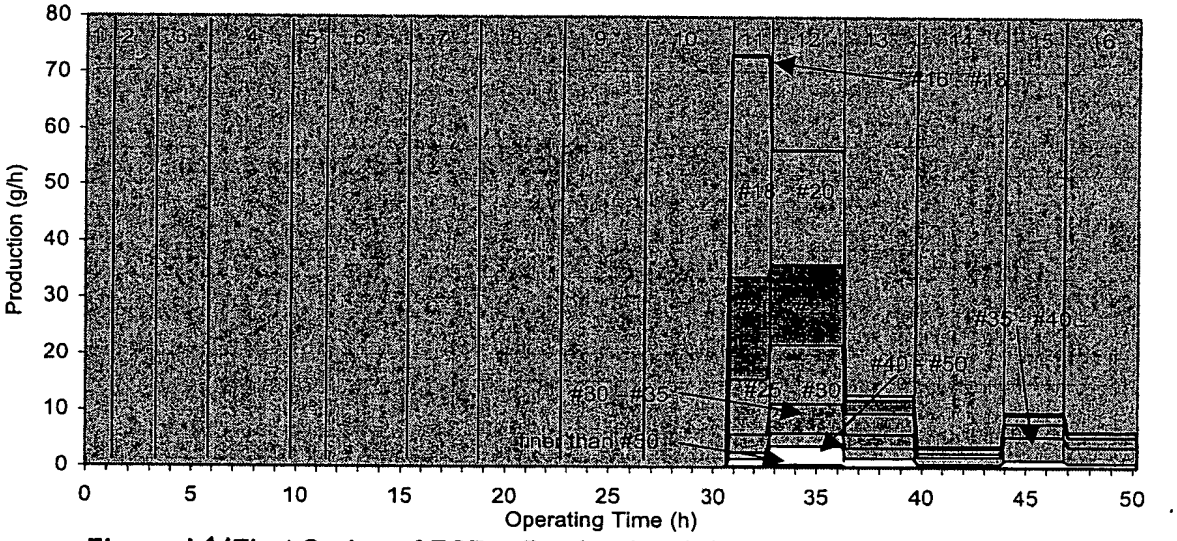

Figure 14: First Series of FCRs: Production (g/h), Averaged Over Each Run, Broken Down by Particle Size (Standard Sieve)
(Numbered Vertical Strips Correspond with Runs)

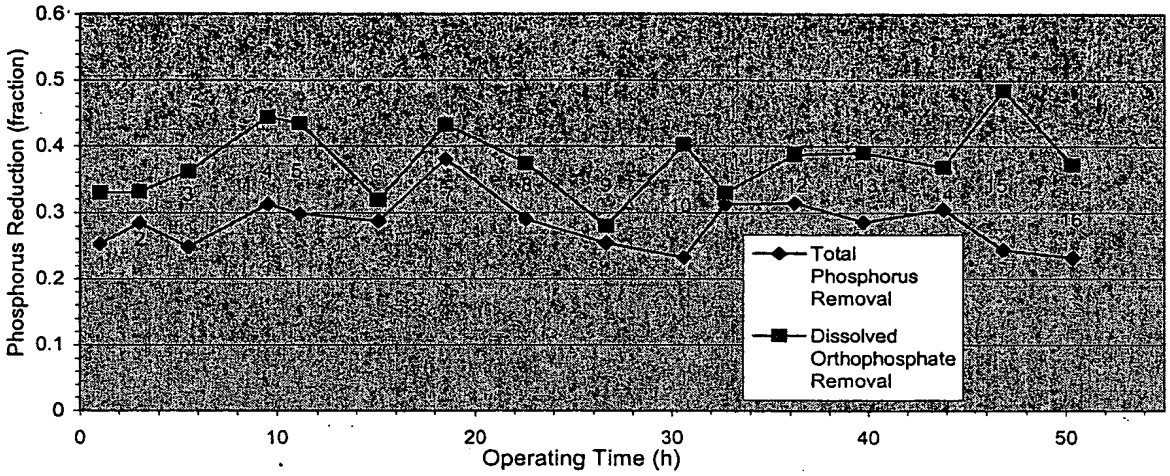

Figure 15: First Series of FCRs: Phosphorus Reduction (fraction) vs. Operating Time (h)
(Run Numbers Indicated)

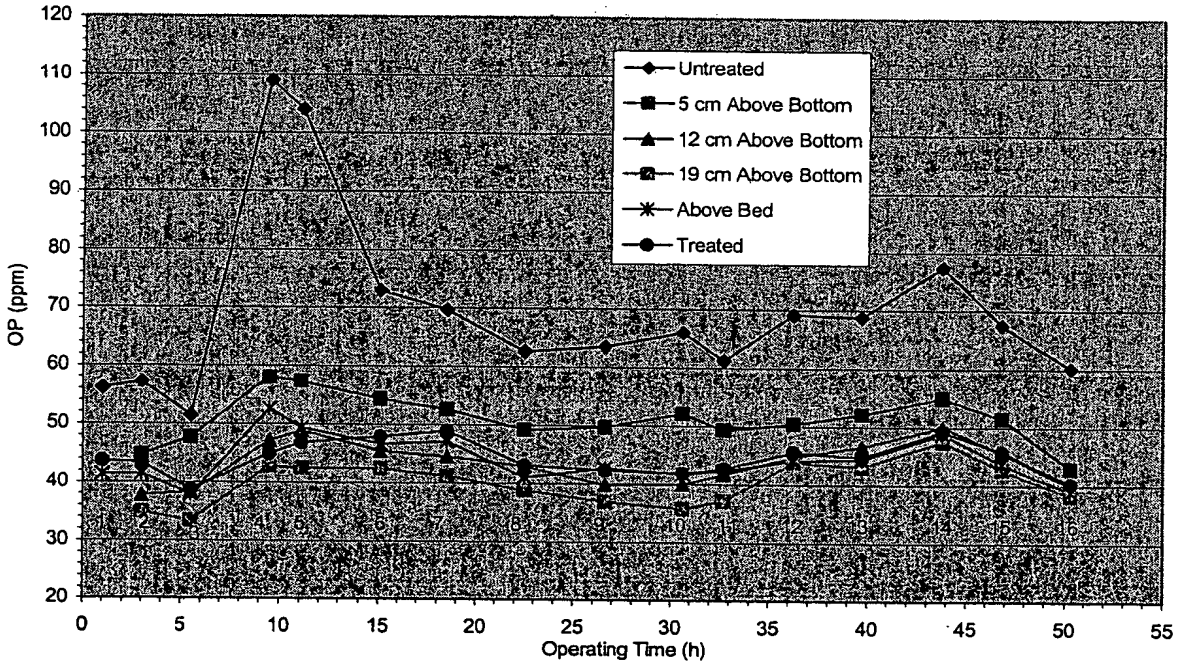

Figure 16: First Series of FCRs: OP (ppm) at Various Sampling Points vs. Operating Time (h)
(Run Numbers Indicated)

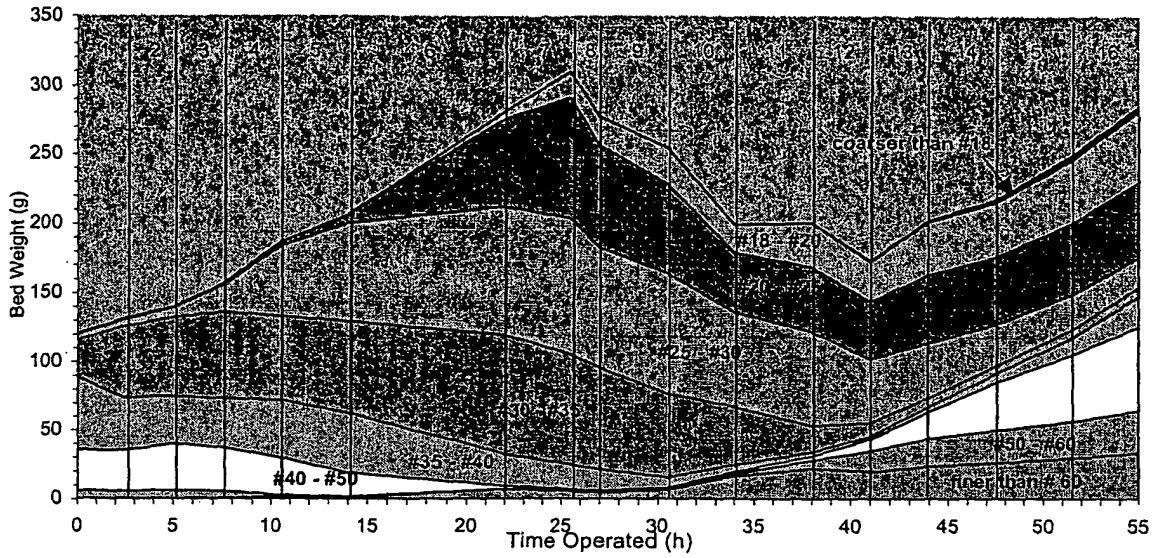

Figure 17: Second Series of FCRs: Bed Weight (g), Broken Down by Particle Size (Standard Sieve), vs. Time Operated (h)
(Numbered Vertical Strips Correspond with Runs)

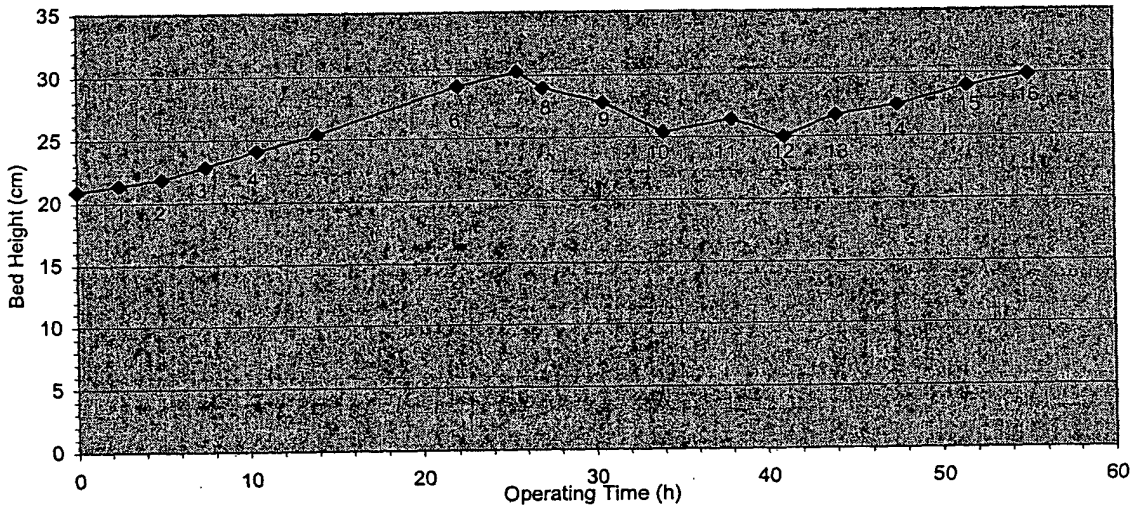

Figure 18: Second Series of FCRs: Bed Height (cm) at End of Run vs. Operating Time (h)
(Run Numbers Indicated)

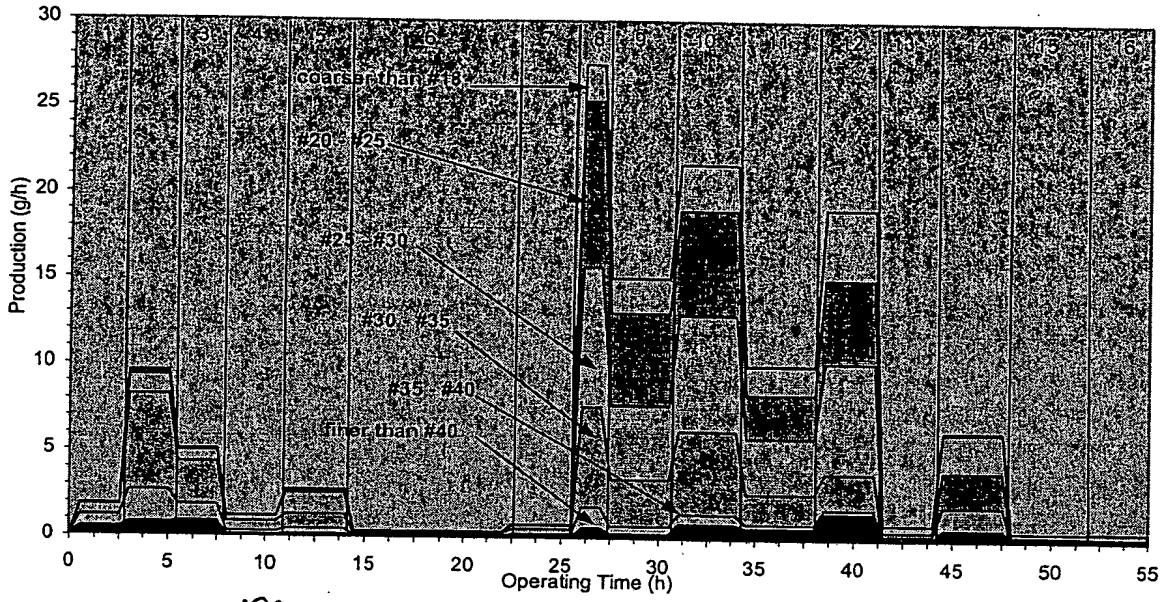

Figure 19: Second Series of FCRs: Production (g/h), Averaged Over Each Run, Broken Down by Particle Size (Standard Sieve)
(Numbered Verticle Strips Correspond with Runs)

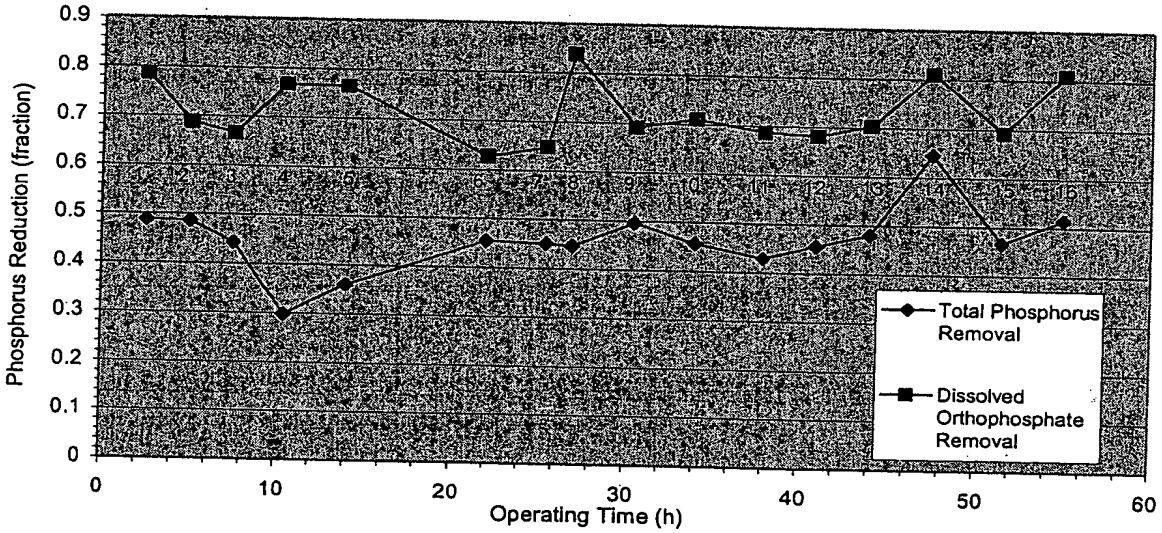

Figure 20: Second Series of FCRs: Phosphorus Reduction (fraction) vs. Operating Time (h)
(Run Numbers Indicated)

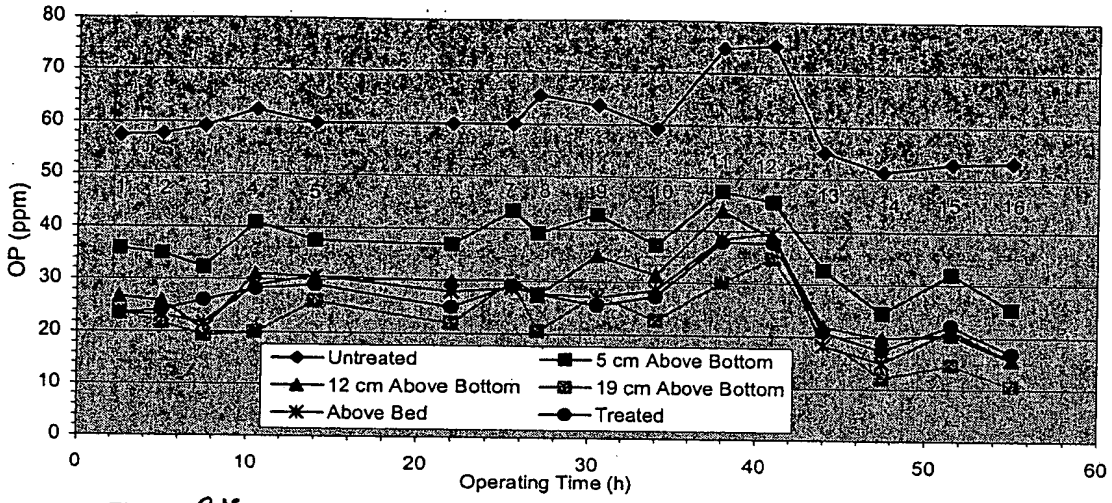

Figure 21: Second Series of FCRs: OP (ppm) at Various Sampling Points vs. Operating Time (h)
(Run Numbers Indicated)

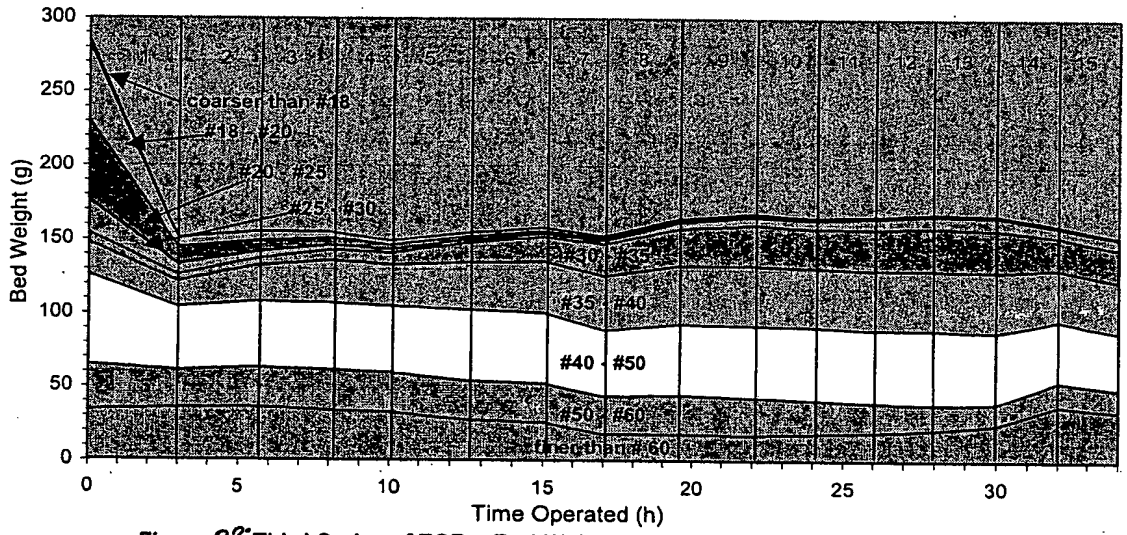

Figure 22: Third Series of FCRs: Bed Weight (g), Broken Down by Particle Size (Standard Sieve), vs. Time Operated (h)
(Numbered Vertical Strips Correspond with Runs)

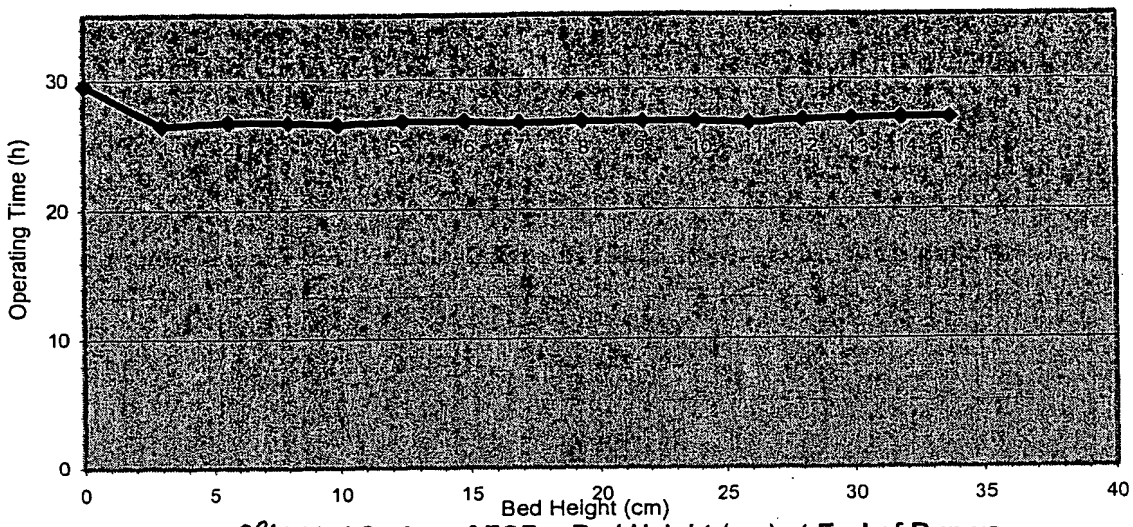

Figure 23: Third Series of FCRs: Bed Height (cm) at End of Run vs. Operating Time (h)
(Run Numbers Indicated)

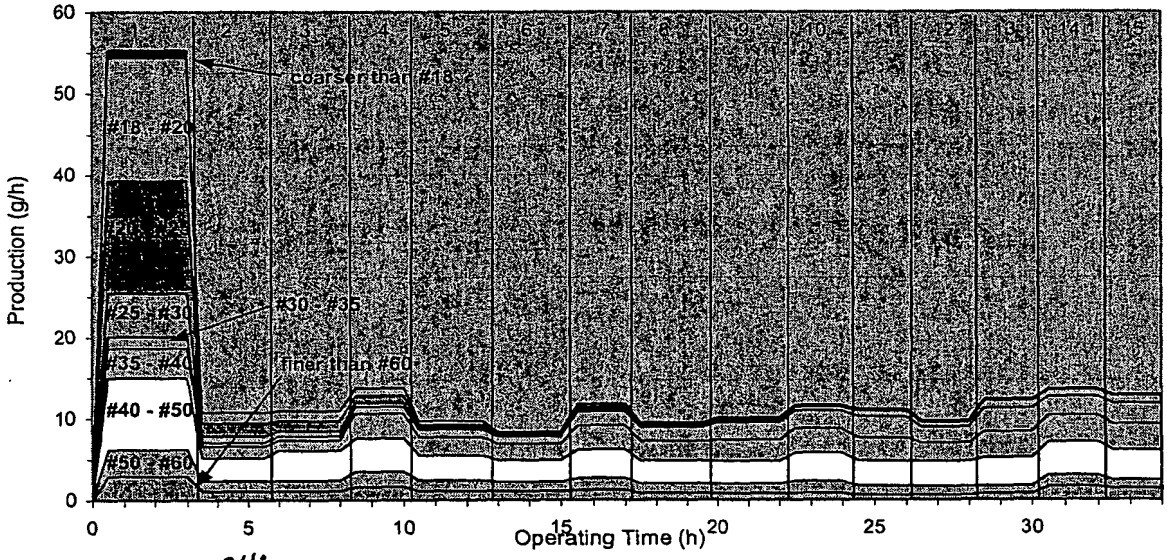

Figure 24: Third Series of FCRs: Production (g/h), Averaged Over Each Run, Broken Down by Particle Size (Standard Sieve)
(Numbered Vertical Strip Correspond with Runs)

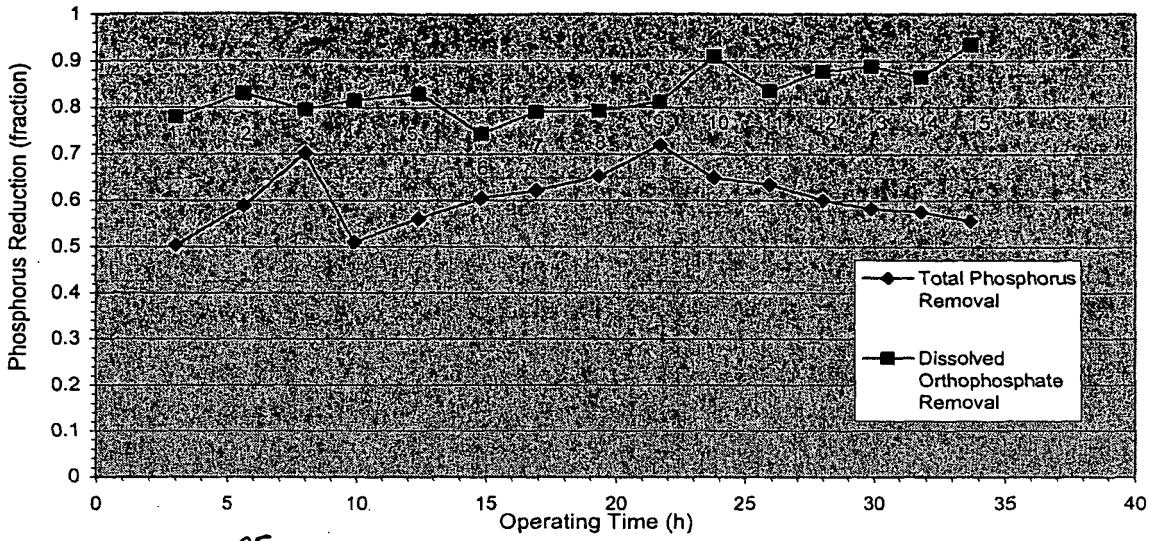

Figure 25: Third Series of FCRs: Phosphorus Reduction (fraction) vs. Operating Time (h)
(Run Numbers Indicated)

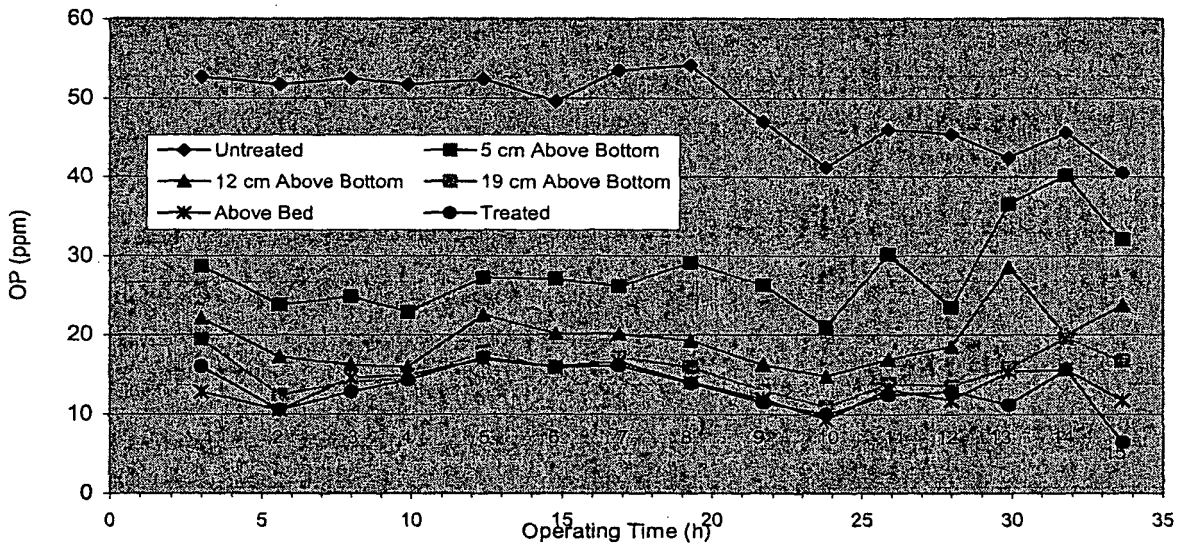

Figure 26: Third Series of FCRs: OP (ppm) at Various Sampling Points vs. Operating Time (h)
(Run Numbers Indicated)

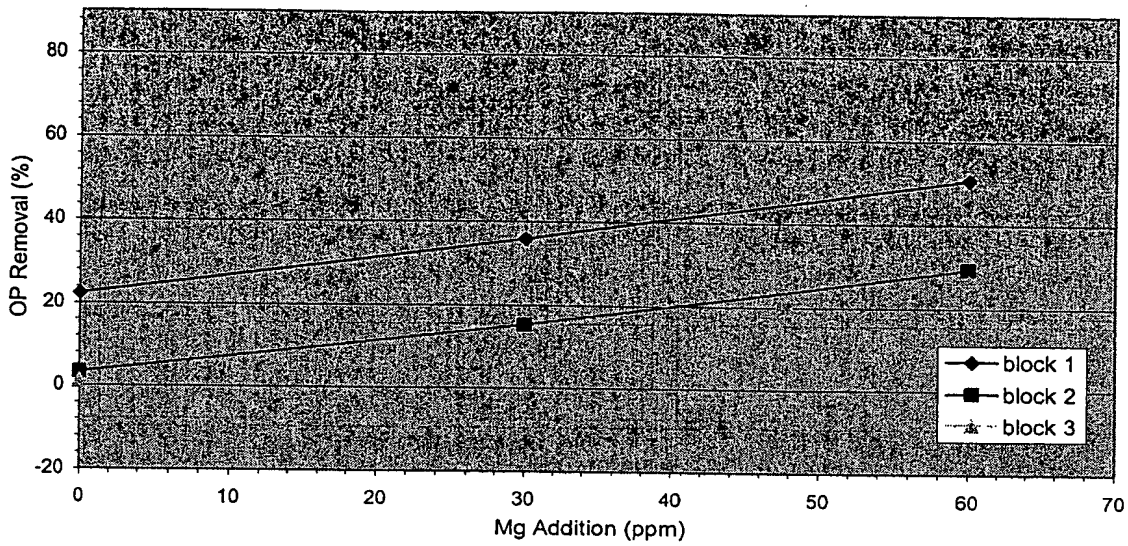

Figure 27: MVRs: OP Removal (%) vs. Mg Addition (ppm) with Zero Ammonia and 41.2 L/h Flow

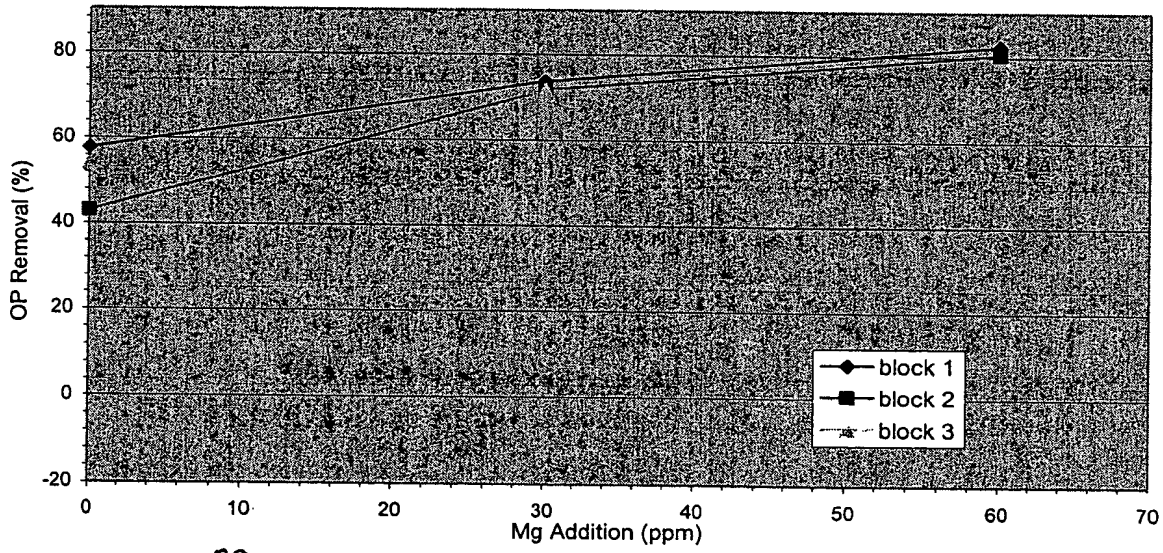

Figure 28: MVRs: OP Removal (%) vs. Mg Addition (ppm) with 100 ppm (as TAN) Ammonia Addition and 41.2 L/h Flow

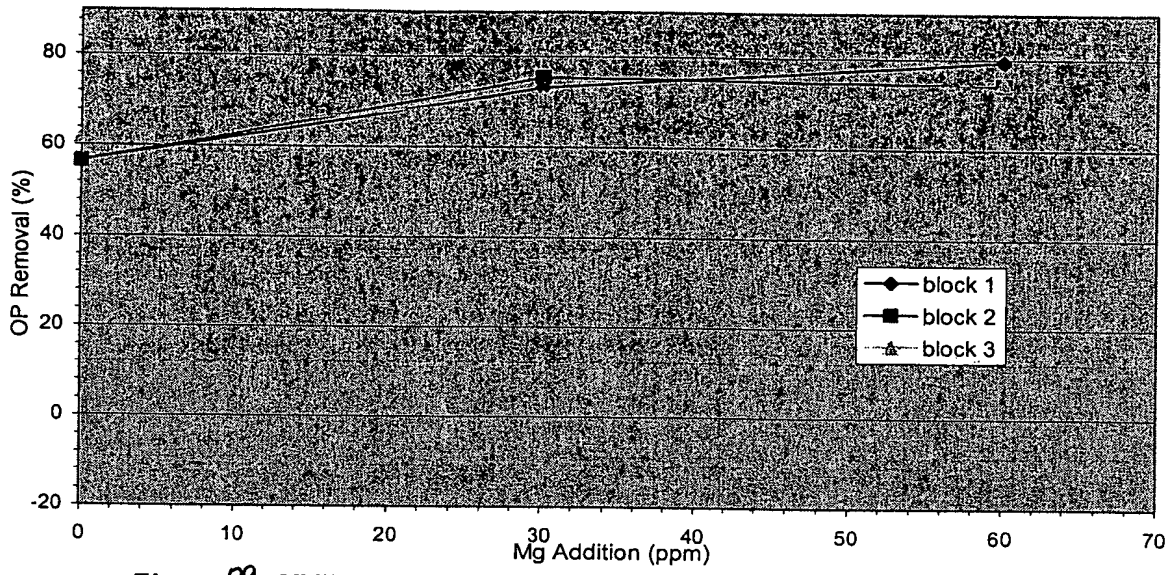

Figure 29: MVRs: OP Removal (%) vs. Mg Addition (ppm) with 200 ppm (as TAN) Ammonia and 41.2 L/h Flow

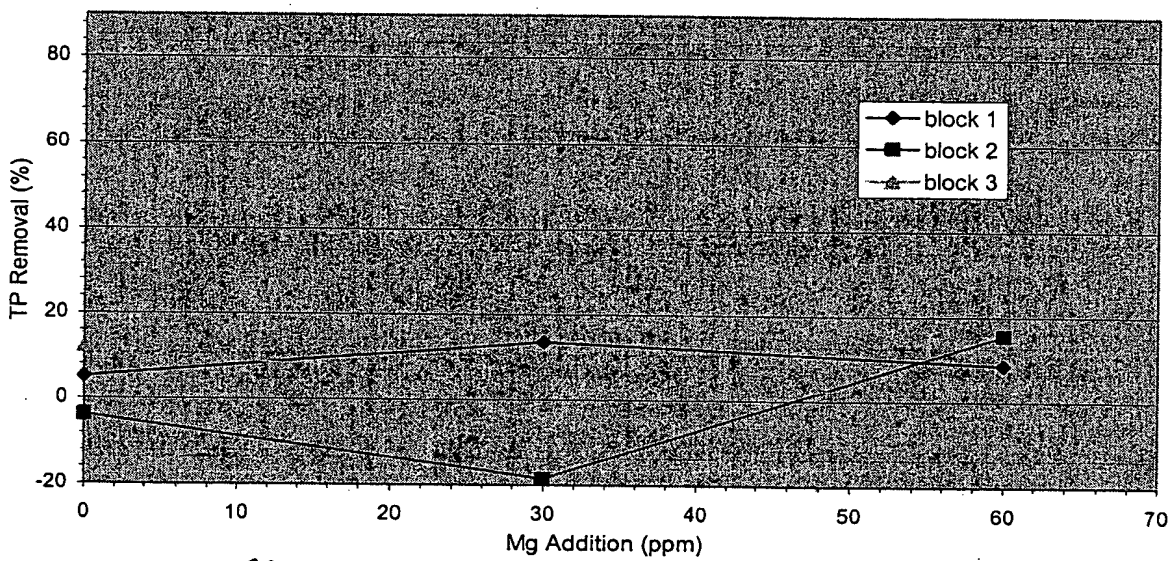

Figure 30: MVRs: TP Removal (%) vs. Mg Addition (ppm) with Zero Ammonia and 41.2 L/h Flow

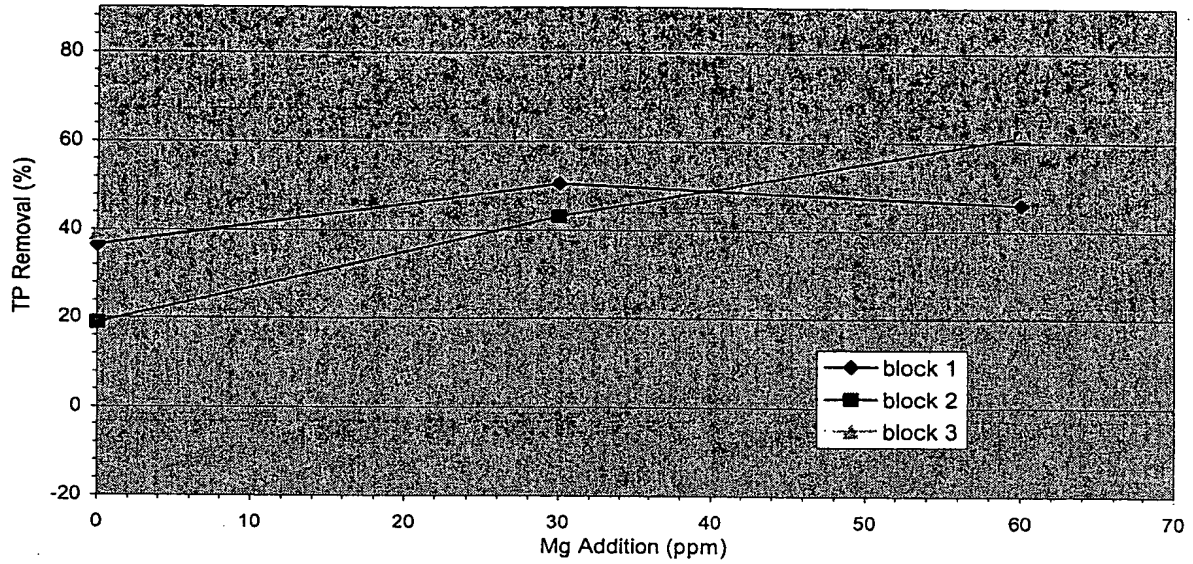

Figure 31: MVRs: TP Removal (%) vs. Mg Addition (ppm) with 100 ppm (as TAN) Ammonia and 41.2 L/h Flow

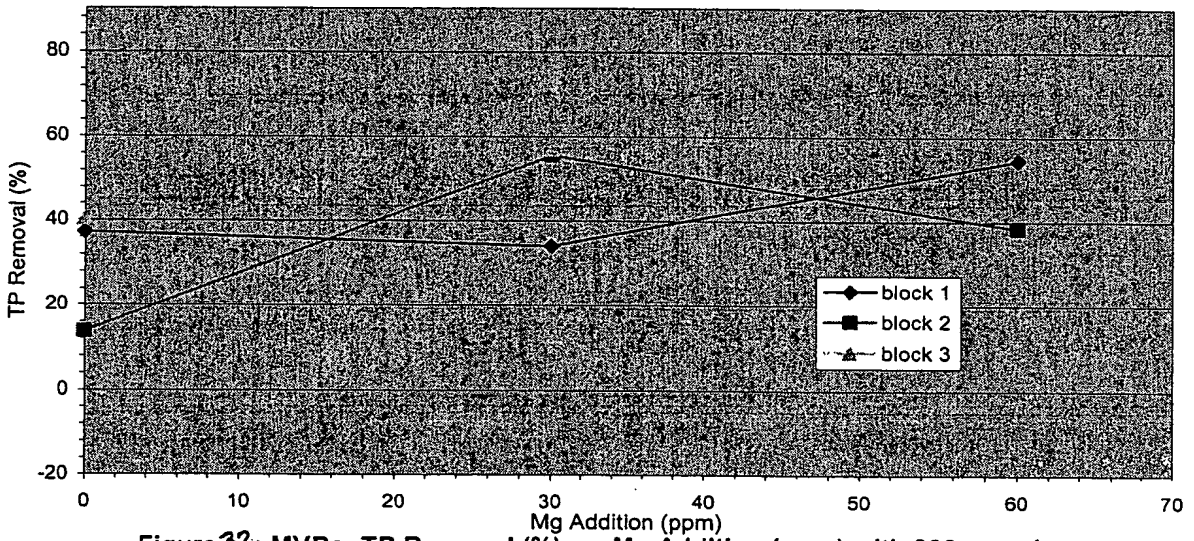

Figure 32: MVRs: TP Removal (%) vs. Mg Addition (ppm) with 200 ppm (as TAN) Ammonia and 41.2 L/h Flow

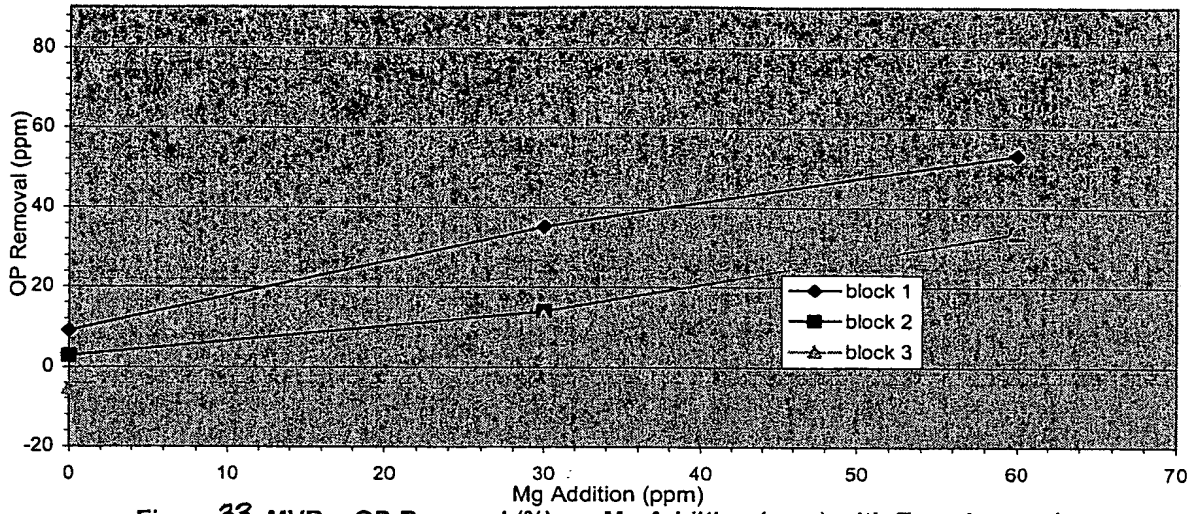

Figure 33: MVRs: OP Removal (%) vs. Mg Addition (ppm) with Zero Ammonia and 56.8 L/h Flow

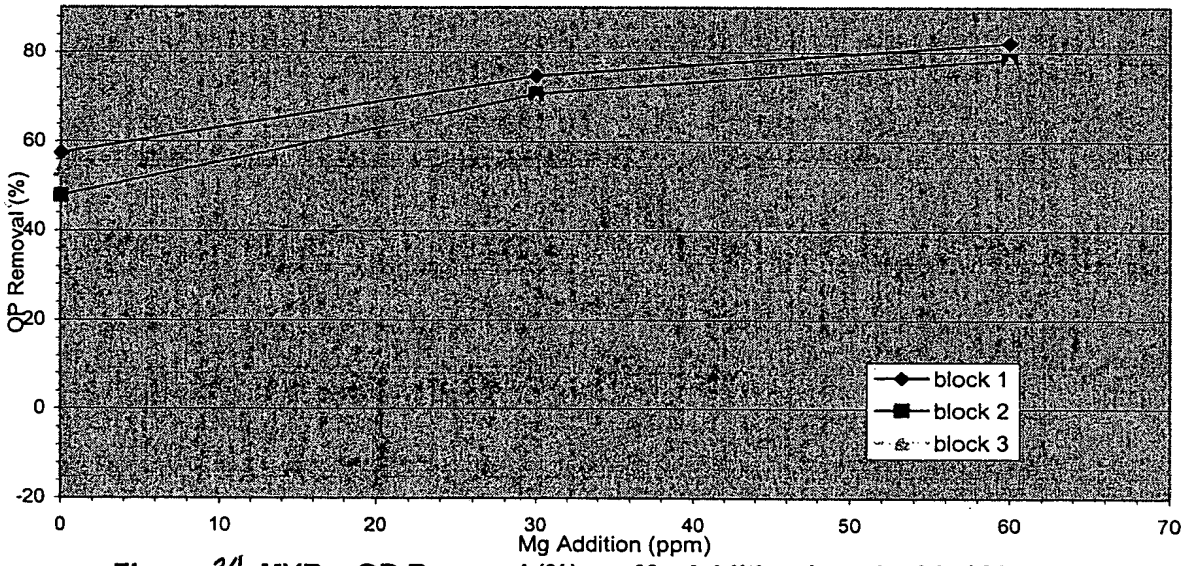

Figure 34: MVRs: OP Removal (%) vs. Mg Addition (ppm) with 100 ppm (as TAN) Ammonia and 56.8 L/h Flow

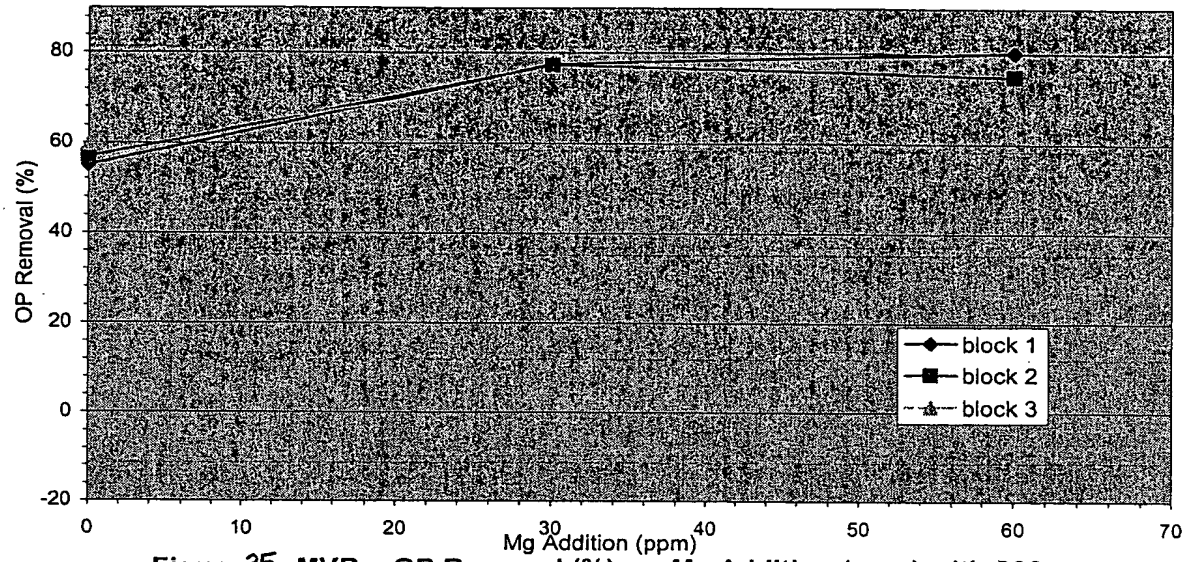

Figure 35: MVRs: OP Removal (%) vs. Mg Addition (ppm) with 200 ppm (as TAN) Ammonia and 56.8 L/h Flow

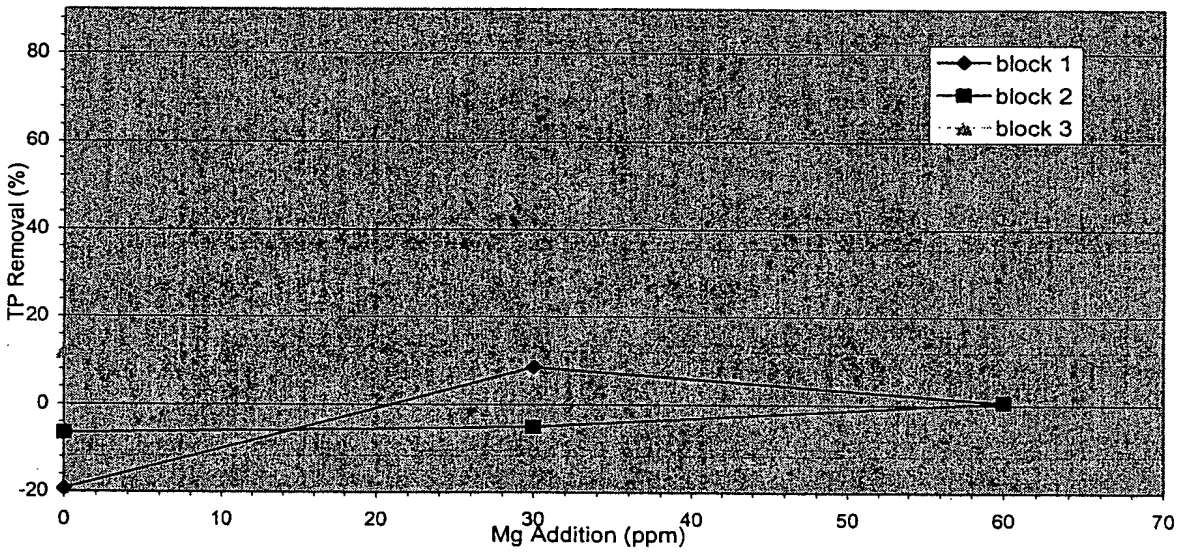

Figure 36: MVRs: TP Removal (%) vs. Mg Addition (ppm) with Zero Ammonia and 56.8 L/h Flow

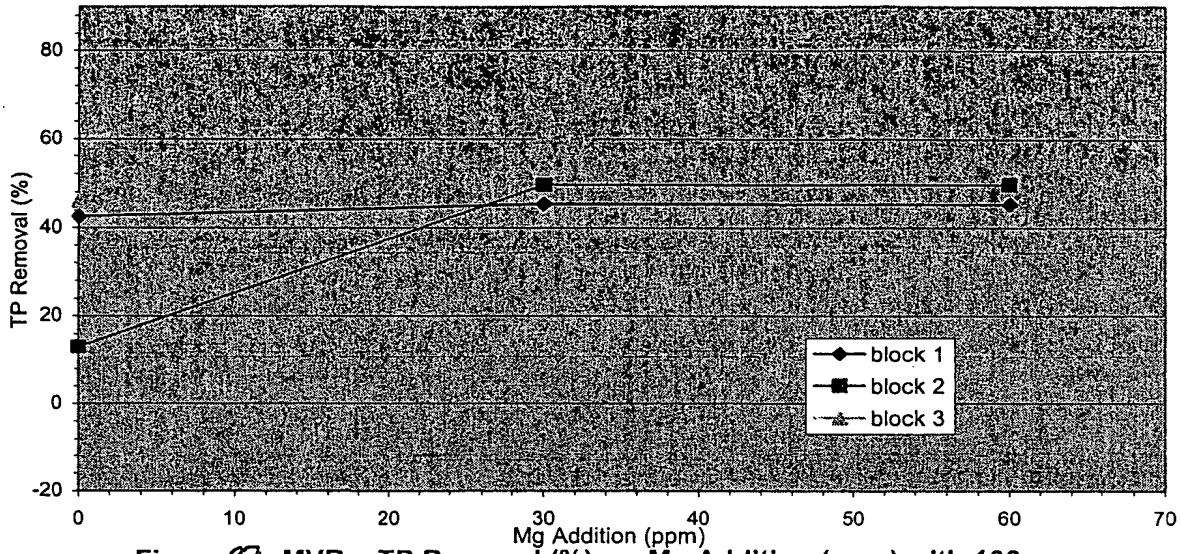

Figure 37: MVRs: TP Removal (%) vs. Mg Addition (ppm) with 100 ppm (as N) Ammonia and 56.8 L/h Flow

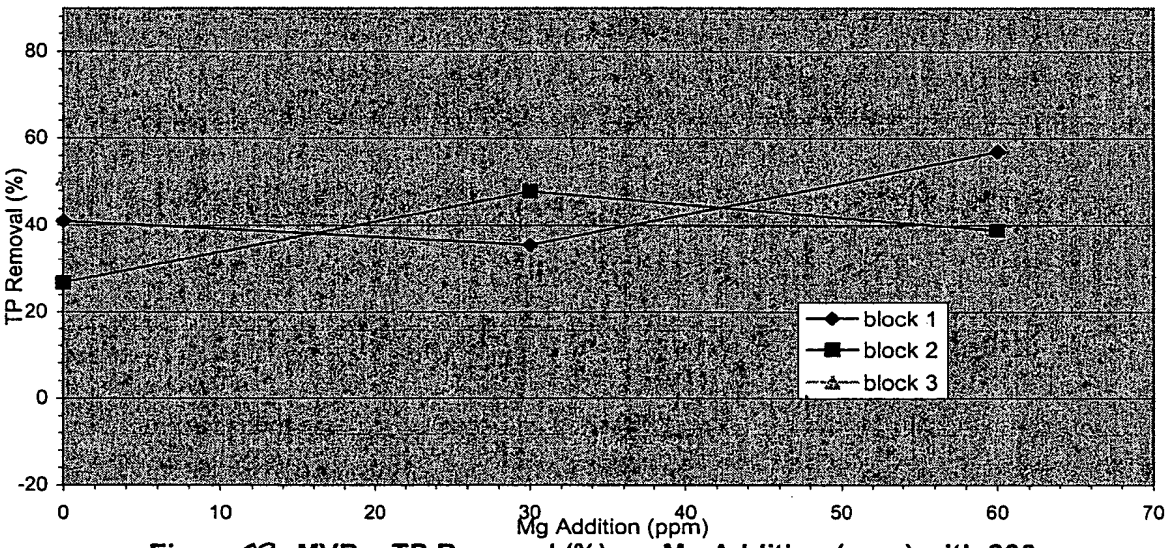

Figure 38: MVRs: TP Removal (%) vs. Mg Addition (ppm) with 200 ppm (as N) Ammonia and 56.8 L/h Flow

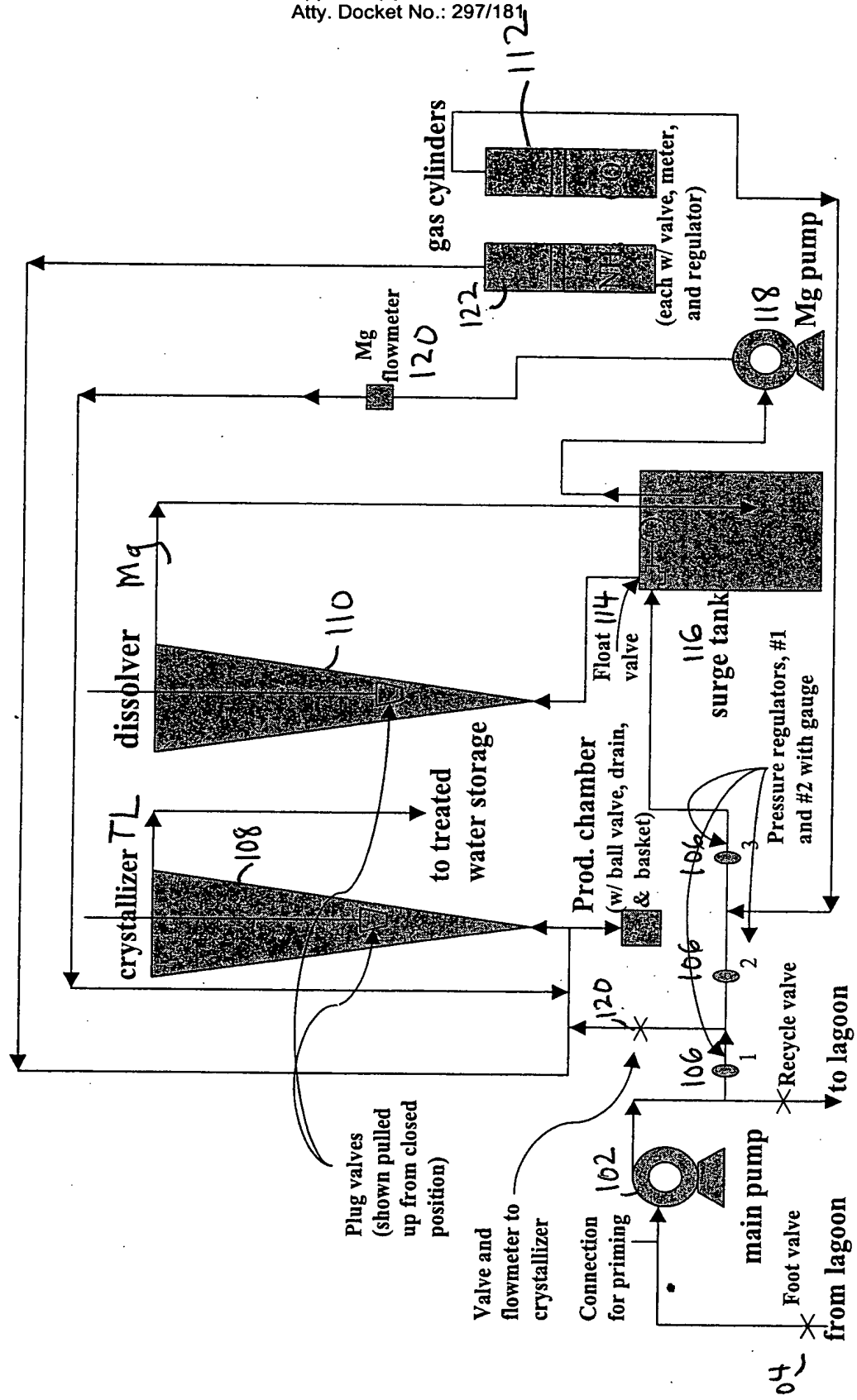

Figure 3: Schematic Representation of Field-Scale Crystallizer, Showing Principal Components

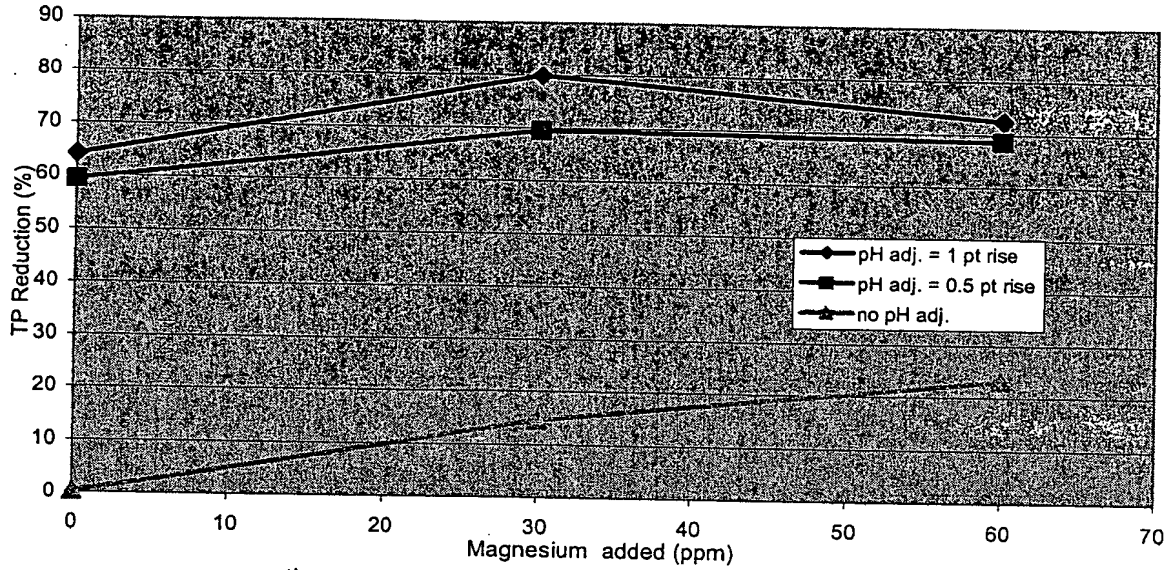

Figure 40: TP Reduction (%) vs. Magnesium added (ppm) at Lower Flow Rate (341 L/h)

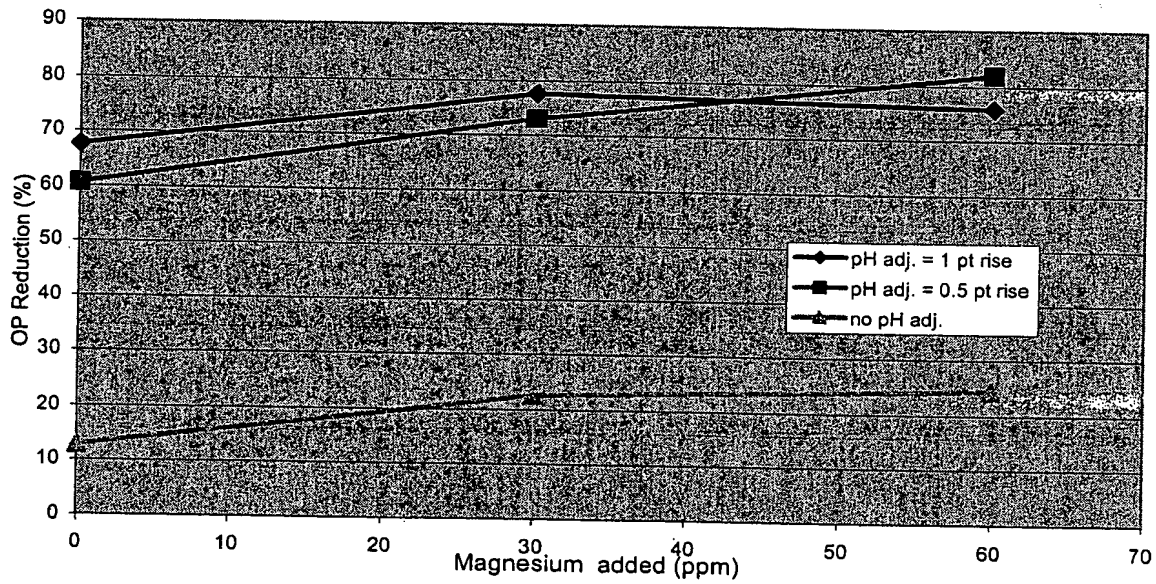

Figure 41: OP Reduction (%) vs. Magnesium added (ppm) at Lower Flow Rate (341 L/h)

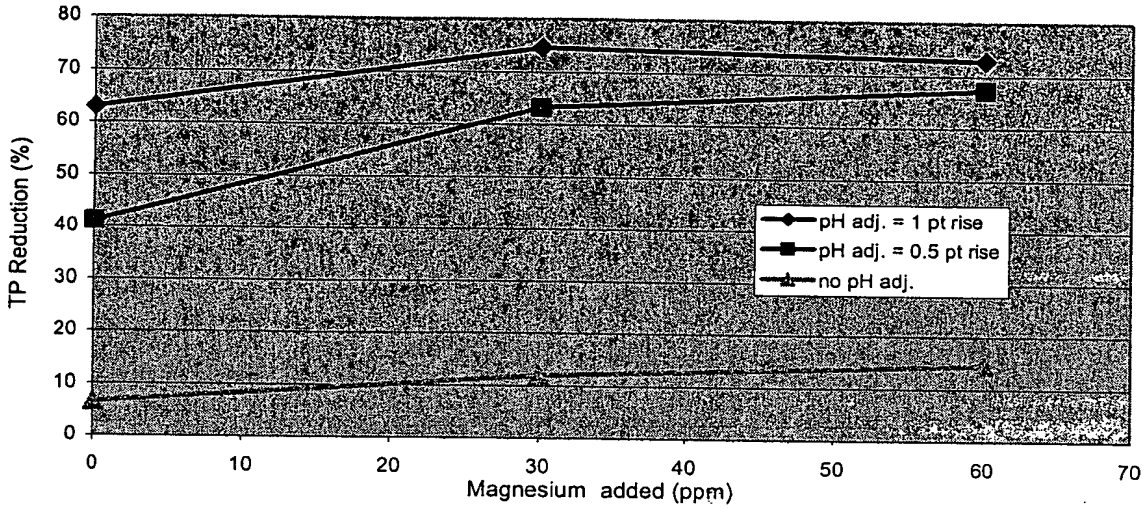

Figure 42: TP Reduction (%) vs. Magnesium added (ppm) at Higher Flow Rate (568 L/h)

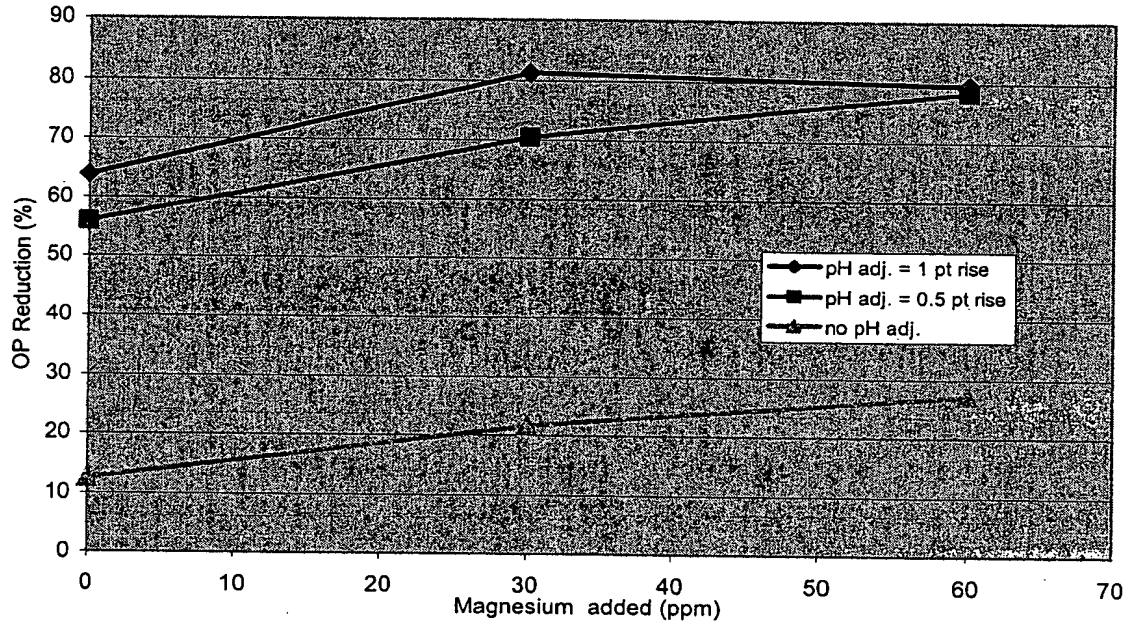

Figure 43: OP Reduction (%) vs. Magnesium added (ppm) at Higher Flow Rate (568 L/h)